# Plasma enhanced chemical vapor deposition of silicon oxide films using TMOS/O$_2$ gas and plasma diagnostics

S.B. Bang, T.H. Chung*, Y. Kim

*Department of Physics, Dong-A University, Hadan-dong 840, Saha-Gu, Busan 604-714, South Korea*

## Abstract

Thin oxide films are deposited from tetramethoxysilane in an inductively coupled oxygen glow discharge supplied with radio frequency power. The deposition rate and the chemical bonding states of deposited films are analyzed by ellipsometry and by Fourier transform infrared spectroscopy, respectively, and the intensities of light emission from molecules and radicals in the plasma are measured by optical emission spectroscopy. Langmuir probe is employed to estimate the plasma density and electron temperature. With these tools, the effects of parameters such as r.f. power of inductive coupling, substrate bias power, oxygen partial pressure ratio, total pressure on the properties of the film and of the plasma are investigated. The correlation between the properties of the film and the characteristics of the plasma are explained wherever possible.
© 2003 Elsevier B.V. All rights reserved.

## 1. Introduction

Silicon dioxide is commonly used as interlayer dielectrics in integrated circuits and microelectronics devices. When the substrate materials have poor heat resistance, it is necessary to deposit silicon oxide at low temperature. Plasma enhanced chemical vapor deposition (PECVD) allows to deposit good quality films at low substrate temperature.

Although silane is widely used as a silicon precursor, organosilicon sources such as TMOS (tetramethoxysilane), TEOS (tetraethoxysilane) and HMDSO (hexamethyldisiloxane) deposited with an oxidizer are much better for the conformal thin films which are used in inter-metal dielectrics. PECVD of silicon dioxide from organosilicon sources and oxygen plasma has been extensively investigated [1–7]. However, the deposition mechanism of silicon oxide at low temperature is not elucidated. The primary issues have been how process conditions such as silicon precursor dilution and pressure, power govern film deposition and composition.

In PECVD, the plasma is used as an aid to chemically decompose the vapor precursor and as a source of active species involved in the film growth. Therefore, accurate plasma diagnostics enable not only the understanding of the deposition process but also better control of the deposited film properties [8]. The energy of deposition is controlled by the electric field at the surface of the growing film. By applying an electrical bias to the substrate one can control the energetic growth conditions of a PECVD film. Low-temperature deposition by PECVD becomes practical when combined with ion bombardment during the film growth. Ion bombardment induces changes in the film density and composition similar to high deposition temperature. Film density and hardness increases as sputtering removes the weakly bonded material.

This paper deals with the deposition of SiO$_2$ thin films in TMOS/O$_2$ inductively coupled r.f. plasma. Inductively coupled plasma (ICP) source can provide a high-density plasma, which has been utilized widely for PECVD, and it can control the ion flux and the ion bombardment energy separately with the substrate r.f. bias. The controllability of bombardment energy can help to find the optimal process condition for PECVD.

*Corresponding author. Tel.: +82-51-200-7228; fax: +82-51-200-7232.

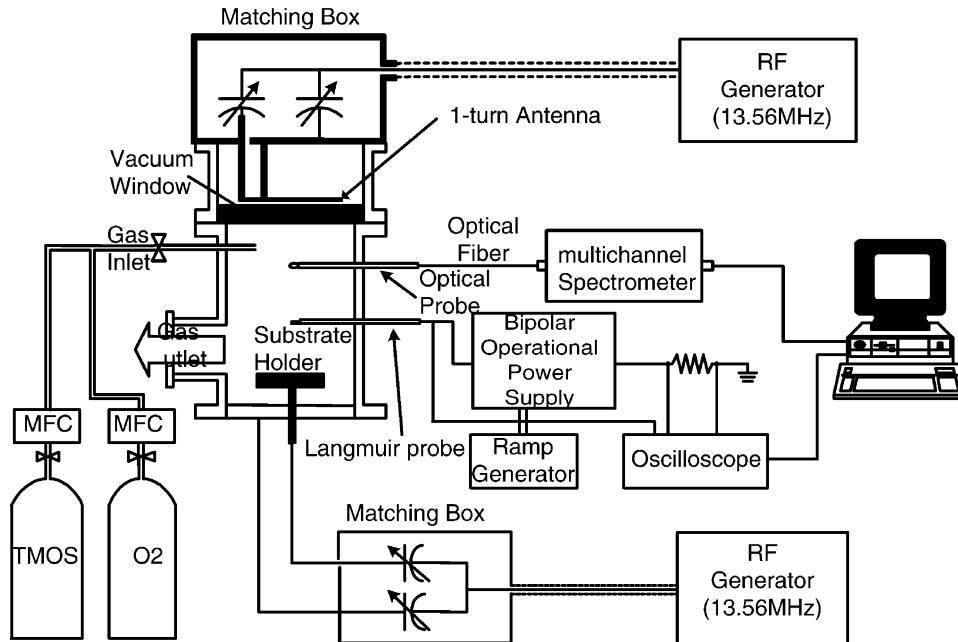*E-mail address:* thchung@plasma.donga.ac.kr (T.H. Chung).

Fig. 1. Schematic diagram of the ICP PECVD system with plasma diagnostic.

Diagnostics of the excited and charged species of the plasma by optical emission spectroscopy (OES) and Langmuir probes are carried out simultaneously with the characterization of the $SiO_2$ layers in ex-situ by Fourier transform infrared spectroscopy (FTIR) and by ex-situ ellipsometry. OES is an in-situ non-intrusive analytic technique for monitoring the chemical species in various plasmas. It can be used to investigate the reaction mechanisms for PECVD process, since the precursor decomposition produces a large number of emissive species, which contribute significantly to the determination of film properties.

The aim of this paper is to study the effect of various process parameters such as ICP power, oxygen partial pressure ratio, substrate bias power and total gas pressure on the characteristics of the plasma and on the properties of the deposited film.

## 2. Experiments

The PECVD reactor utilizes an inductively coupled plasma source operating at 13.56 MHz to sustain low-pressure (1–50 mTorr) high-density plasmas. Oxygen gas flow and TMOS, regulated by mass flow controller (AFC 50), are introduced approximately 10 cm above the substrate. Films are deposited on p-type Si (100) substrate.

The schematic diagram of this system is shown in Fig. 1. The plasma chamber consists of a stainless-steel cylinder with 28-cm diameter and 34-cm length. A 1.9-cm thick by 27-cm diameter tempered glass plate mounted on one end separates a planar one-turn induction coil

from the plasma. The induction coil is made of copper (with water-cooling) and connected to an L-type capacitive matching network and a r.f. power generator (ENI OEM-12). To control the ion bombardment energy, the electrode on which the substrate is placed can be independently driven by a capacitively coupled r.f. source. Hence, independent control of the ion/radical fluxes (through the ICP power) and the ion bombardment energy (through the substrate bias power) is possible.
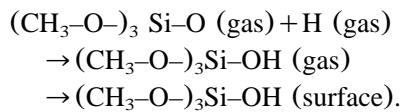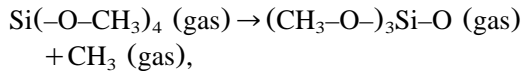
The partial pressure of an organosilicon compound and that of oxygen gas were controlled by mass flow controllers. The parameter $R$ is defined as the ratio of the partial pressure of the oxygen gas to the total pressure $R = p_{O_2}/p_{total}$. We varied the total pressure from 1 to 50 mTorr, the ICP power from 100 to 600 W, the substrate bias power from 0 to 60 W and the $R$ from 0 to 0.9.

The chemical bonding states of deposited films were analyzed by FTIR (BIO RAD Excalibur). The light intensities of emissive gaseous species in the plasma were collected by an optical fiber that was coupled to multi-channel spectrometer (OPC-2000). Emission light from glow discharge is detected through a home-made optical probe during deposition in the wavelength range of 250–700 nm with a resolution of 1 nm. The dependence of the emission intensities on process parameters is investigated. The thickness of deposited $SiO_2$ layer is measured using the ellipsometer (Gaertner Scientific L117). The incidence angle is 70° and the wavelength is 632 nm.

A Langmuir probe system is built to determine the density and the electron temperature of the plasma. The Langmuir probe was powered by a bipolar operational power supply amplifier (Kepco, Inc.). A triangular ramp wave, swept from $-50$ to $+50$ V at 300 Hz was fed into the amplifier from a function generator (Model AFG320, Tektronix Ltd.). The Langmuir probe tip was made of tungsten and located 10 cm above the substrate. The current measurement is done across a 200 $\Omega$ resistor placed between the common and ground outputs of the amplifier. The current and voltage signals are collected on a HP54645A digitizing oscilloscope. During deposition, the probe tip was contaminated due to the deposition of insulating film. Between scan, the probe tip was cleaned by electron bombardment by pulse biasing it to $+150$ V.

## 3. Results and discussion

The mechanism of the formation of film from organosilicon precursor such as TMOS has been suggested. Inoue et al. have shown that the formation mechanism of Si–O–Si bond is based on dehydration condensation from silanol group as follows [1]:

$$Si(-O-CH_3)_4 \text{ (gas)} \rightarrow (CH_3-O-)_3Si-O \text{ (gas)} + CH_3 \text{ (gas)},$$

$$(CH_3-O-)_3 Si-O \text{ (gas)} + H \text{ (gas)}$$
$$\rightarrow (CH_3-O-)_3Si-OH \text{ (gas)}$$
$$\rightarrow (CH_3-O-)_3Si-OH \text{ (surface)}.$$

Then, with the extraction of $H_2O$ and methyl function, silicon oxide films are formed. This route is called the ion-induced pathway. However, mass spectroscopy study revealed that TMOS molecules are almost completely broken into small radicals such as SiO and $CH_n$ in the r.f. plasma [9]. The Si–O–Si network is formed from the surface reactions of these fragments. Another suggested mechanism is

$$Si(-O-CH_3)_4 + 7\ O \rightarrow SiO_2 + 2\ CO_2 + 2\ CO + 3\ H_2O + 3\ H_2,$$
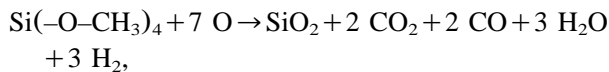
which is called oxygen atom-induced pathway [10]. Combining these two pathways, it can be stated that neutral oxygen atoms and $O_2^+$ ions react with adsorbed TMOS fragments to produce $SiO_2$ and volatile by-products [11]. In this study, the deposition process was described based on the above proposed models.

Deposition studies were carried out as functions of the ICP power ($P_p$), substrate bias r.f. power ($P_s$), $O_2$ partial pressure ratio ($R$) and total gas pressure ($p_{total}$). The deposition rate was determined by the ratio of the film thickness to the deposition time. It is important to
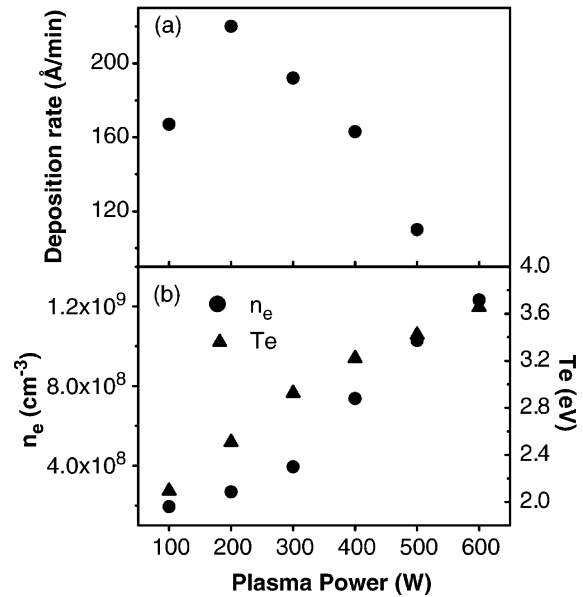


Fig. 2. (a) Deposition rate and (b) electron density and electron temperature as a function of ICP power, where $P_s = 30$ W, $R = 0.4$, $p_{total} = 10$ mTorr.

understand how chemically activated species move from the gas phase to the film surface because their rate of arrival determines the deposition rate. Neutral radicals created in the plasma find their way to the surface of the film by diffusion. The ICP power supplied to plasma determines how many electrons activate the gas (electron density) and how hard they work (electron energy).

As can be seen in Fig. 2a, the deposition rate starts increasing with the ICP power, reaches a maximum and drops down to very low values for high ICP power. This result is in contrast to usual observation where the deposition rate rises until a critical power above, which it saturates. An increasing deposition rate with the ICP power can be explained by an enhanced generation of precursors and radicals. In Fig. 2b, the electron density and electron temperature are displayed with varying ICP power. Since the ICP power provides an effective activation energy for ionization and heating of gas, the increase of ICP power results in the increase of electron density and electron temperature. A larger ICP power results in high ion-flux, which promotes an etching of the deposited film. Therefore, the deposition rate decreases again with increasing ICP power.

A typical emission spectrum of the inductively coupled TMOS/$O_2$ plasma is shown in Fig. 3. Optical emission spectroscopy measurements revealed the strong emission features of $H_\alpha$(656 nm), $H_\beta$(486 nm), $H_\delta$(410 nm), $H_\gamma$(434 nm), OH (285 and 306 nm), CO (266 nm), CH (431 nm), $C_2$ (516.5 nm), $O_2^+$ (360, 525 and 563 nm). The emission spectra are dominated by the strong emissions of excited H, OH, $C_2$, CH, O and $O_2^+$.
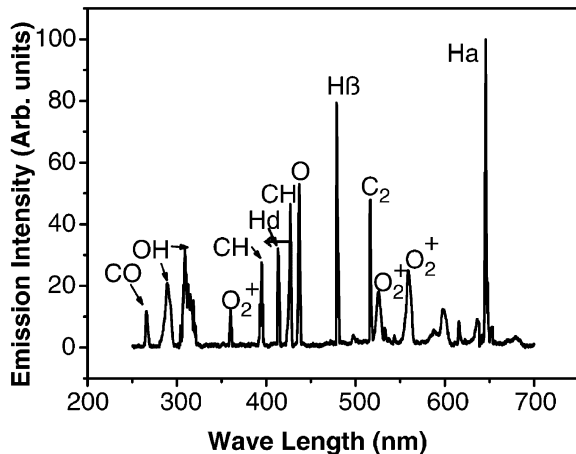
Fig. 3. Optical emission spectrum ranging from 250 to 700 nm of TMOS/$O_2$ plasma, where $P_p = 400$ W, $P_s = 30$ W, $R = 0.4$, $p_{total} = 10$ mTorr.

They can be classified into two categories depending on whether they are from TMOS molecular dissociation (CH, H) or chemical reactions of atoms composing TMOS among themselves ($C_2$, $H_2$) or from the oxygen of the plasma (O, $O_2^+$, OH). No emissions from any species containing Si are observed, suggesting that TMOS molecule is not completely dissociated in the plasma. The same phenomenon was observed in TEOS/$O_2$ plasma [4], but they were detected in HMDSO/$O_2$ plasma [12].

Although not shown in figures, we observe that the intensities of all the above-mentioned lines increase with increasing ICP power and decrease with increasing pressure. As the substrate bias power increases, the intensities increase up to a certain level and then saturate.

In Fig. 4a, the dependence of the deposition rate on oxygen fraction $R$ is displayed. The ICP power, substrate bias power, and pressure are kept constant at 400 W, 30 W and 20 mTorr, respectively. Starting from TMOS only case ($R = 0$), the deposition rate increases with an addition of oxygen, which probably promotes gas-phase decomposition of the monomer molecules and a formation of intermediate precursors. The deposition rate shows a maximum at $R = 0.4$. This is caused by a balance between the amount of atomic oxygen needed to convert TMOS in the film and the amount of TMOS supplying the material for the film growth. For high $O_2$ fraction, the deposition rate is limited by the availability of TMOS, while for low $O_2$ fraction, the surface is covered with the fragments of TMOS and the rate limiting comes from the availability of O atoms. When $R$ is near one (higher oxygen fraction), the characteristics of the plasma should be largely controlled by oxygen excitation/de-excitation. The TMOS molecules are not dramatically dissociated in the plasma. A similar trend

is found in the case of TEOS [12], but this behavior is in contrast to the case of HMDSO where the deposition rate is linearly-dependent on HMDSO concentration [13]. It should be noted that too much bombardment of active oxygen molecules (large $R$ case) can cause more serious damage when polymer substrates are used [14]. Note that the values of the deposition rate are less than those obtained in reactors utilizing microwave plasma source [15].

Fig. 4b shows the evolution of peaks of H, CH and OH as a function of $R$. The difference in the sensitivity of the spectrometer in the spectral range used is not taken into consideration. When $R$ is small, the fragmentation of the monomer is mainly by an electron impact. As $R$ increases the electron density and the density of oxygen atoms increase. Then they contribute to the fragmentation of the monomer and the TMOS precursors. Near and above $R = 0.5$, the densities of electron and oxygen atom are high enough to dissociate the monomer, there are high fragments of TMOS precursors (H, CH, OH). The high intensity of hydrogen Balmer series was also observed in HMDSO/$O_2$ discharge [15]. With larger $O_2$ fraction, $H_2$ molecules are dissociated into H atoms and part of these atoms react with oxygen to yield OH radical [15]. The emission intensities from CH and atomic H drastically increase with the number of methyl functions in reactant molecules [1]. This region is called a high-monomer-fragmentation regime [15]. However, when $R$ is too high (near 100%) the quantity of the TMOS monomer decreases drastically, therefore, the emission line intensities decrease.
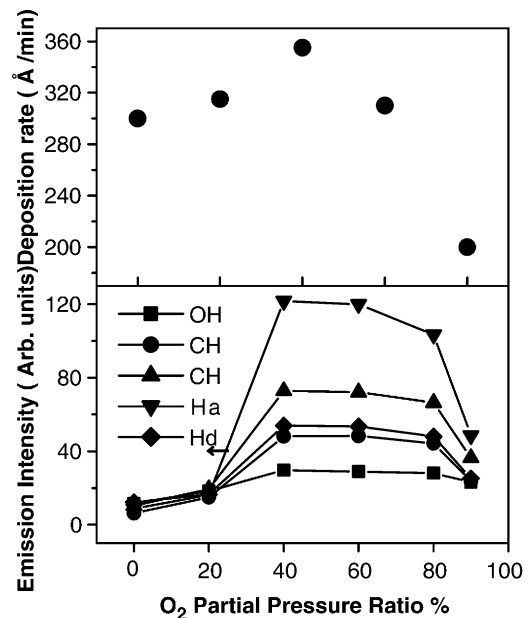


Fig. 4. (a) Deposition rate and (b) various emission line intensities as a function of oxygen fraction $R$, where $P_p = 400$ W, $P_s = 30$ W, $p_{total} = 10$ mTorr.
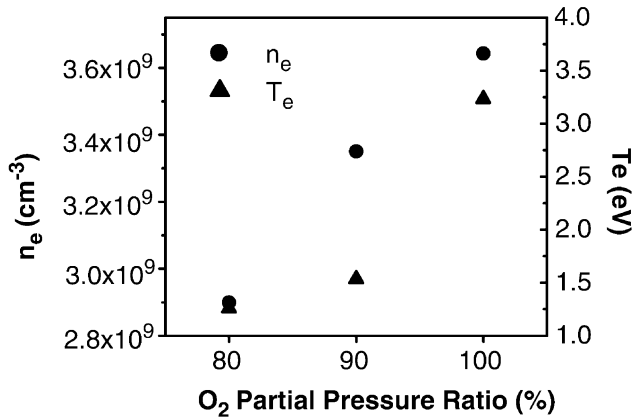
Fig. 5. The variation of electron density and electron temperature with oxygen partial pressure ratio. $P_p = 400$ W, $P_s = 20$ W, $p_{total} = 20$ mTorr.

The variations of the electron density and electron temperature are shown in Fig. 5 as a function of oxygen partial pressure ratio at 20 mTorr and ICP power of 400 W and the substrate power of 20 W. The electron temperature increases with $R$. The relative abundance of TMOS goes along with a decrease in the number of high-energy electron. The dissociation of TMOS acts as a cooling process for the electron gas. With larger $R$, one observes an increase in the electron density, which results from direct ionization of oxygen molecules and oxygen atoms. Although not shown in figures, the electron temperature decreases with the total pressure.

Fig. 6a shows the change of the deposition rate as a function of substrate bias power. The deposition rate increases with increasing substrate bias power up to 50 W and then decreases slightly. The ion bombardment due to substrate r.f. bias activates the gas in the substrate vicinity and surface adsorption sites, leading to a net adsorption rate higher than the case of a pure ICP plasma [16]. A larger substrate bias power than 50 W facilitates the etching of the deposited film, thus is harmful to the deposition rate. Fig. 6b shows the variation of electron density and electron temperature with substrate bias power. With increasing substrate bias power, the electron density and electron temperature increase. Dual mode operation of inductive and capacitive coupling seems to enhance the gas activation. As in the case of dual ECR-r.f. discharge of methane [17], the substrate r.f. biasing does not only induce ion acceleration but also enhances the electron density and electron temperature. The contribution of hot electrons in the presence of r.f. biasing may lead to enhancement of ionization and dissociation processes of TMOS [17]. It should be noted that we cannot control the substrate bias power independently of the other plasma parameters. The bias affects the electron density and electron temperature, which again affect the ion density and radical density. The substrate bias power larger than 60
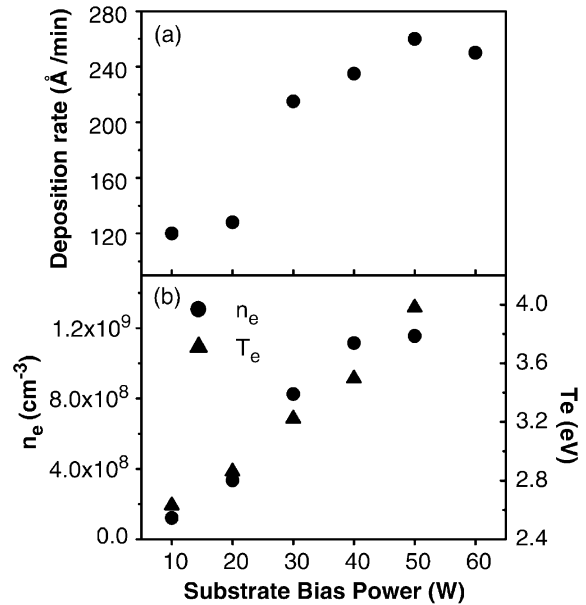


Fig. 6. (a) Deposition rate and (b) electron density and electron temperature as a function of substrate bias power, where $P_p = 400$ W, $R = 0.4$, $p_{total} = 10$ mTorr.

W results in capacitive discharge near the substrate and changes the plasma properties. At this power level, the discharge becomes unstable and the probe $I$–$V$ data obtained shows a low degree of credibility, thus the data point is not shown. It should be mentioned that a film can be deposited without substrate bias power (ICP mode only). However, the films deposited under the only ICP mode exhibit poor properties in film density and hardness.

Fig. 7 shows the dependence of the deposition rate on the total gas pressure. With increasing gas pressure, the deposition rate increases until 40 mTorr and then it decreases. The decrease in the deposition rate with increasing pressure is due to lower electron density and lower atomic oxygen density, which are caused by infrequent dissociation. The abundance of oxygen atom
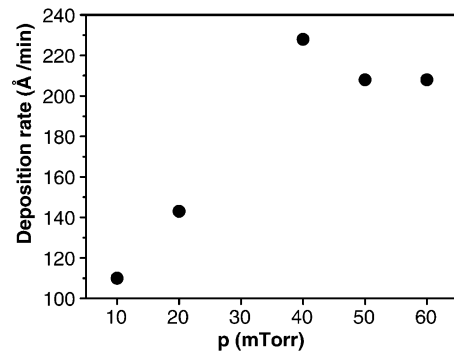


Fig. 7. Deposition rate as a function of total pressure, where $P_p = 500$ W, $P_s = 30$ W, $R = 0.4$.
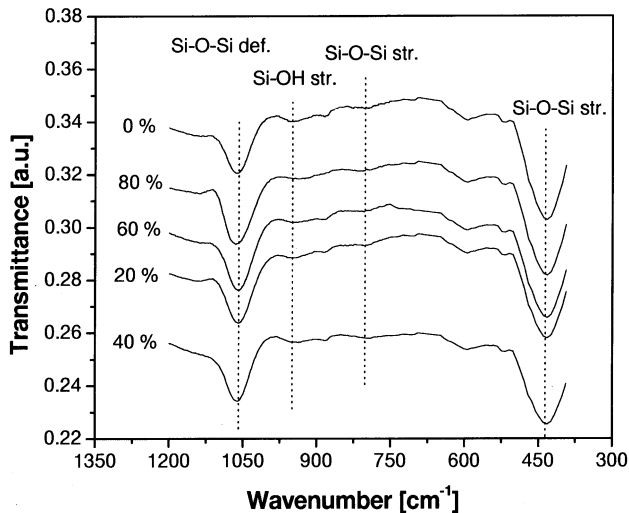
Fig. 8. FTIR transmission spectra for the films deposited at various oxygen partial pressure ratios, where $P_p = 600$ W, $P_s = 20$ W, $p_{total} = 30$ mTorr.

is proportional to the electron density since oxygen atoms are created mainly by the dissociation of $O_2$ by electron impact. Since the deposition rate depends on a sum of the oxygen atom-induced pathway and the ion-induced pathway, the contributions from both pathways have a similar dependence on total pressure.

Fig. 8 presents the FTIR spectra obtained from films deposited with varying oxygen partial pressure ratio. The FTIR spectra exhibit absorption peaks corresponding to Si–O–Si stretching at 1062 cm$^{-1}$, Si–OH stretching at 950 cm$^{-1}$, Si–O–Si deformation at 796 cm$^{-1}$. A small absorption band is detected approximately 870–760 cm$^{-1}$, which is due to Si–CH$_3$ rocking. Another small absorption band is detected approximately 1280–1250 cm$^{-1}$, which are due to Si–CH$_3$ symmetric deformation. In addition, absorption peaks appear approximately 1360–1330 cm$^{-1}$, which are due to the environment moisture. The Si–O–Si stretching peak at 450 cm$^{-1}$ is also observed. The IR spectra of the films show a weak $R$-dependence and are similar to the spectrum of pure silicon dioxide except for the bands due to Si–OH bonds and CH groups [1]. As oxygen fraction is increased, absorption peak due to Si–OH bond increases slightly. However, as $R$ approaches 1.0, the absorption peak slowly decreases again. The remaining Si–OH bands in the deposited film are due to the low substrate temperature. This residual Si–OH bands reduces the electrical resistivity and degrade the mechanical properties. We observe that the OH intensity and hydrogen Balmer lines intensities (seen in Figs. 3 and 4) follow the same trends as the OH absorbance measured by FTIR. This behavior was also observed in the case of TEOS/O$_2$ [3,6]. The correlation between emission of OH and the presence of OH in the film is

observed. It should be noted that since the conditions required for actinometry are not fulfilled, these intensities could not be considered as proportional to ground state density. However, these intensities are expected to be correlated with the chemical composition of the plasma and the deposition kinetics.

The wavenumber of Si–O–Si stretching mode in the entire $R$ range was approximately 1055–1065 cm$^{-1}$, which is lower than that of thermal oxide (1075 cm$^{-1}$). The vibration wavenumber depends on the Si–O–Si bond angle. Since the change of the bond angle at different $R$ is negligible, the change in $R$ does not influence the microstructure of the deposited film, which was also observed in the thin film deposited from TEOS/O$_2$ discharge [18]. The Si–O–Si stretching peak slowly decreases with decreasing $R$ (increasing TMOS flow rate) [19].

In Fig. 9, we observe that as the substrate bias power increases the Si–OH peak decreases. It was observed that an r.f. bias applied to the substrate decreased the entire SiOH integrated absorbance in the microwave CVD reactor [16]. It has been also observed that higher power level of capacitively coupled PECVD system decreased the Si–OH peaks [20]. The OH elimination is achieved due to the temperature increase of the substrate at higher substrate power. PECVD films always contain precursor fragments such as hydrocarbon group. It is possible to minimize their concentration by raising the substrate temperature or by increasing the degree of ion bombardment during deposition. High ion fluxes at low ion energies (25–50 eV) are particularly useful in this respect.

## 4. Conclusions

Plasma enhanced chemical vapor deposition of silicon dioxide thin films using inductively coupled r.f. dis-
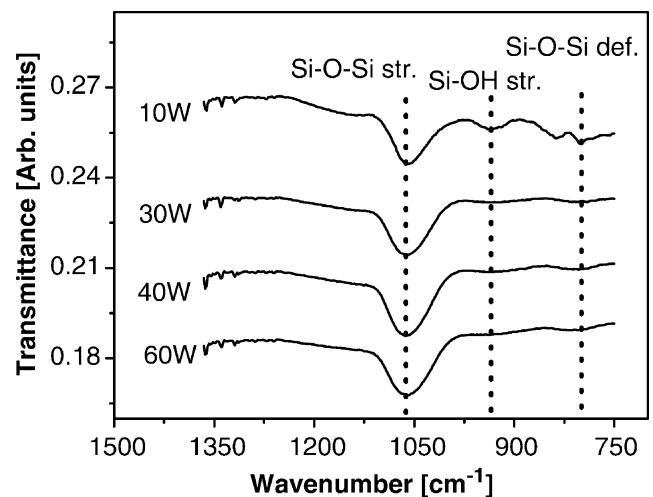


Fig. 9. FTIR transmission spectra for the films deposited at various substrate bias powers, where $P_p = 400$ W, $R = 0.5$, $p_{total} = 10$ mTorr.

charge of tetramethoxysilane and oxygen plasma was investigated. The composition of the plasma and the characteristics of the deposited films have been studied with varying process parameters. The process parameters such as ICP power, oxygen partial pressure ratio, substrate bias power and total gas pressure had profound effect on the deposition rate and the film quality. From the evolution of the deposition rate and of the plasma characteristics as functions of operating parameters and by considering the chemical bonding states of the obtained thin films, the proposed models of the ion-induced pathway and the oxygen atom-induced pathway can explain the deposition mechanism. Especially, it is found that oxygen atoms promote the dissociation of TMOS molecules and play an important role in the deposition process. However, the oxygen partial pressure ratio should be restricted in a proper value. Identifying the nature of the fragments responsible for the film deposition and explaining the correlation between the plasma properties and the film properties in more detailed manner will be a subject of further study.

## Acknowledgments

## References

[1] Y. Inoue, O. Takai, Plasma Sources Sci. Technol. 5 (1996) 339.

[2] Y. Inoue, O. Takai, Thin Solid Films 341 (1999) 47.

[3] F. Nicolazo, A. Goullet, A. Granier, C. Vallee, G. Turban, B. Grolleau, Surf. Coat. Technol. 98 (1998) 1578.

[4] K. Aumaille, A. Granier, M. Schmidt, B. Grolleau, C. Vallee, G. Turban, Plasma Sources Sci. Technol. 9 (2000) 331.

[5] R. Mota, D. Galvao, S.F. Durrant, M. Moraes, S. Dantas, M. Cantao, Thin Solid Films 270 (1995) 109.

[6] S.C. Deshmukh, E.S. Aydil, J. Vac. Sci. Technol. B 14 (1996) 738.

[7] A. Grill, V. Patel, J. Appl. Phys. 85 (1999) 3314.

[8] B. Cho, S. Lao, L. Sha, J.P. Chang, J. Vac. Sci. Technol. A 19 (2001) 2751.

[9] Y. Inoue, O. Takai, Thin Solid Films 316 (1998) 79.

[10] G.B. Raupp, T.S. Cale, H.P.W. Hey, J. Vac. Sci. Technol. B 10 (1992) 37.

[11] D.F. Richards, M.O. Bloomfield, S. Soukane, T.S. Cale, Vacuum 59 (2000) 168.

[12] K. Aumaille, C. Vallee, A. Granier, A. Goullet, F. Grolleau, G. Turban, Thin Solid Films 359 (2000) 188.

[13] J.A. Theil, J.G. Brace, R.W. Knoll, J. Vac. Sci. Technol. A 12 (1994) 1365.

[14] Y. Inoue, H. Sugimura, O. Takai, Thin Solid Films 345 (1999) 90.

[15] N. Benissad, C. Boisse-Laporte, C. Vallee, A. Granier, A. Goullet, Surf. Coat. Technol. 116–119 (1999) 868.

[16] N. Benissad, K. Aumaille, A. Granier, A. Goullet, Thin Solid Films 394 (2001) 230.

[17] J. Hong, A. Granier, C. Leteinturier, M.-C. Peignon, G. Turban, J. Vac. Sci. Technol. A 18 (2000) 497.

[18] H.U. Kim, S.W. Rhee, J. Mater. Sci.: Mater. Electron. 11 (2000) 579.

[19] C. Vallee, A. Goullet, F. Nicolazo, A. Granier, G. Turban, J. Non-Cryst. Solids 216 (1997) 48.

[20] K. Teshima, Y. Inoue, H. Sugimura, O. Takai, Vacuum 66 (2002) 353.